

Stability Analyses and Design Recommendations for Practical Shoring Systems during Construction

Jui-Lin Peng¹

Abstract: This paper presents stability analysis and design recommendations for the falsework of wood and metal post shores. Based on the setup of shoring systems used on actual construction sites, analysis models of the shoring system have been derived. The experimental test results indicate that the base stiffness to the ground of shores is 50 t-cm/rad for (490 kN-cm/rad) wood post shores and 70 t-cm/rad (686 kN-cm/rad) for metal post shores of which the joint stiffness between members is 750 t-cm/rad (7,355 kN-cm/rad). With these stiffnesses, factors of 0.75 for wood post shores and 0.85 for metal post shores are used to modify the critical loads of shoring systems calculated from individual shores. The critical loads of a shoring system increase with the number of fixed strong shores, but are not affected by the number of leaning columns. In simplifying shore design, the LeMessurier formula is used for the strength computation of shoring systems composed of wood post shores. The critical loads of shoring systems increase linearly with the number of strong shores, but they are invariant with the positions of strong shores. If the required number of strong shores is defined, the critical loads of shoring systems can be found by interpolation.

DOI: 10.1061/(ASCE)0733-9364(2002)128:6(536)

CE Database keywords: Falsework; Stability; Shoring; Critical load.

Introduction

Based on surveys of construction accidents (Council 1997), the inadequacy of structural and stability strength is the main cause for collapse of falsework during construction. In construction, most reinforced concrete buildings with headroom of 4–5 m use one-layer post shores as the falsework to support construction loads. These loads arise from fresh concrete, crews, formwork, steel, and so on. In Taiwan, two kinds of shores, wood post shores and metal post shores (i.e., telescopic props), are most widely used in construction (Fig. 1). In general, metal post shores have two parts—a base tube with a threaded collar and a staff tube of smaller diameter fitting into the base. Round tubes are typically used in Taiwan, although square hollow sections are occasionally used. Wood post shores are typically square and are used for shoring and reshoring, like metal post shores.

The criteria used over the past 20 years are not appropriate for current high headroom construction, which has increased considerably in the past few decades. On construction sites in Taiwan, the installation of these one-layer shores is always based on the experience of the workers, since temporary structures are generally considered of secondary importance. The one-layer installation of these shores has a potential danger in construction. An example of collapse for this kind of falsework is shown in Fig. 2.

¹Associate Professor, Dept. of Construction Engineering, Yunlin Univ. of Science and Technology, Touliu, Yunlin, 640 Taiwan, Republic of China.

Note. Discussion open until May 1, 2003. Separate discussions must be submitted for individual papers. To extend the closing date by one month, a written request must be filed with the ASCE Managing Editor. The manuscript for this paper was submitted for review and possible publication on September 7, 1999; approved on December 4, 2001. This paper is part of the *Journal of Construction Engineering and Management*, Vol. 128, No. 6, December 1, 2002. ©ASCE, ISSN 0733-9364/2002/6-536–544/\$8.00+\$0.50 per page.

Previous research on post shores has mainly focused on shoring and reshoring for multistory concrete buildings (Chen and Mosallam 1991; El-Shahhat et al. 1994). For scaffold falsework, the writer and colleagues investigated falsework safety during construction (Peng et al. 1996, 1997). This falsework is typically used in structures with headroom greater than 8 m. For buildings with headroom of 4–5 m, the research on single-layer shores used in construction is limited. Lateral bracings typically used in the one-layer shoring systems are not considered in the study, since the materials of the lateral bracings and their fastened conditions by workers are varied. A lower bound shoring system without lateral bracings is considered in this preliminary research. The safe use of these falsework systems is a goal of the present research.

Research Objectives

This paper investigates stability analysis and design guidelines of one-layer falsework systems of wood and metal post shores. The load-carrying capacity of the shoring systems can be found by comparing analytical results with experimental verification. The objectives of this paper can be summarized as follows:

- To investigate the end stiffness of individual shores,
- To determine the modification factor and to formulate a simple design process for shoring systems,
- To simplify three-dimensional (3D) models to two-dimensional (2D) models,
- To investigate the effect of leaning columns in shoring systems and suggest their design strength, and
- To investigate the effect of numbers and positions of strong shores in a shoring system.

Basic Assumptions and Material Properties

A second-order elastic analysis is used for the numerical calculation in this paper. The equivalent lateral notional disturbing

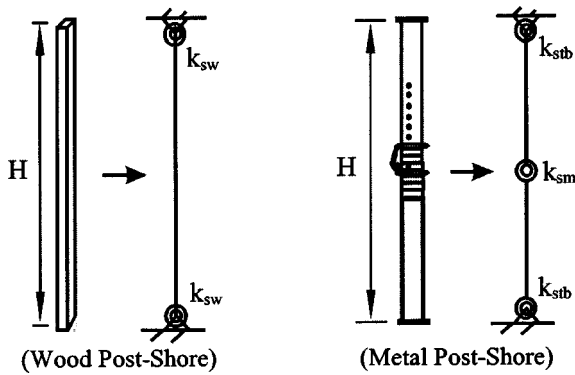


Fig. 1. Individual wood and metal post shore and analysis models

forces, ranging from 0.1 to 0.25% of the total vertical loads in different shoring systems, are adopted to simulate the small initial imperfection with a negligible consideration of residual stresses. The material properties of wood and metal post shores measured from laboratory tests are determined as follows. In wood post shores, the statically flexible elastic modulus is equal to 127.163 t/cm² (12.47 GPa) and the area of the cross section is 32.881 cm². In metal post shores, the elastic modulus is equal to 2,040 t/cm² (200.1 GPa); the area of the cross section for the upper shore (staff tube) is 3.33 cm², and that for the bottom shore (base tube) is 4.02 cm².

Formulations

The proposed second-order elastic analysis in this paper adopts the pointwise equilibrating polynomial element (Chan and Zhou 1994). The element derivation is based on the imposition of compatibility at the end nodes and the satisfaction of equilibrium for the moment and shear at midspan, which is unique in the finite-element context. This element, based on a finite-element formulation, is improved from the cubic Hermite element used in linear analysis.

The basic assumptions in the derivation are listed as follows: (1) The element is prismatic and elastic; (2) the applied loads are conservative and they can be applied at nodes or along the element length; (3) small strain but large deflection is assumed; (4) warping and shear deformation are ignored; and (5) lateral-torsional buckling is neglected for tubular sections.

Six boundary conditions are imposed to evaluate the shape functions of the system. As shown in Fig. 3, four boundary con-



Fig. 2. Collapse of shoring system used in traffic culvert engineering of Southern Second Freeway, Taiwan

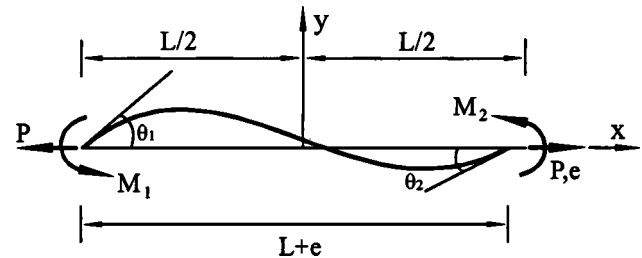


Fig. 3. Basic forces versus displacement relations in element

ditions satisfy the compatibility, as follows:

$$\text{for } x = -L/2; \quad y(-L/2) = 0 \quad \text{and} \quad y'(-L/2) = \theta_1 \quad (1)$$

$$\text{for } x = L/2; \quad y(L/2) = 0 \quad \text{and} \quad y'(L/2) = \theta_2 \quad (2)$$

where a superdot represents differentiation with respect to distance along element x . The remaining two equilibrium conditions for the moment and shear at midspan are listed as follows:

$$EIy'' = Py + \frac{M_2 + M_1}{L}x + \frac{M_2 - M_1}{2} \quad \text{at } x = 0 \quad (3)$$

$$EIy''' = Py' + \frac{M_2 + M_1}{L} \quad \text{at } x = 0 \quad (4)$$

where y = lateral displacement; EI = flexural rigidity; M_1 and M_2 = applied nodal moments at nodes; and L = member length. A fifth-order polynomial y with six unknowns can be found by calculation from Eqs. (1)–(4) as

$$y = a_0 + a_1x + a_2x^2 + a_3x^3 + a_4x^4 + a_5x^5 \quad (5)$$

where y can further be expressed by θ simply as

$$y = (S_1 S_2)(L \theta_1 L \theta_2)^T \quad (6)$$

The two shape functions, S_1 and S_2 , can be derived based on the conditions stipulated in Eqs. (1)–(4), as follows:

$$S_1 = \frac{K_1}{H_1} + \frac{K_2}{H_2} \quad \text{and} \quad S_2 = \frac{K_1}{H_1} - \frac{K_2}{H_2} \quad (7)$$

where

$$K_1 = -20 \frac{x}{L} + \left(80 - \frac{PL^2}{EI} \right) \left(\frac{x}{L} \right)^3 + 4 \left(\frac{PL^2}{EI} \right) \left(\frac{x}{L} \right)^5; \quad H_1 = 80 + \frac{PL^2}{EI} \quad (8)$$

$$K_2 = 6 - \frac{1}{2} \left(48 - \frac{PL^2}{EI} \right) \left(\frac{x}{L} \right)^2 - 2 \left(\frac{PL^2}{EI} \right) \left(\frac{x}{L} \right)^4; \quad H_2 = 48 + \frac{PL^2}{EI} \quad (9)$$

The above shape functions S_1 and S_2 are valid for positive, zero, and negative values of axial force P . In addition, the displacement y will be converted to the cubic Hermite function if the axial force P is zero. The discrepancy between the cubic element and the present fifth-order element increases when the axial force P is large. The present analysis follows a standard Newton-Raphson procedure with improvement by the minimum residual displacement method for convergence.

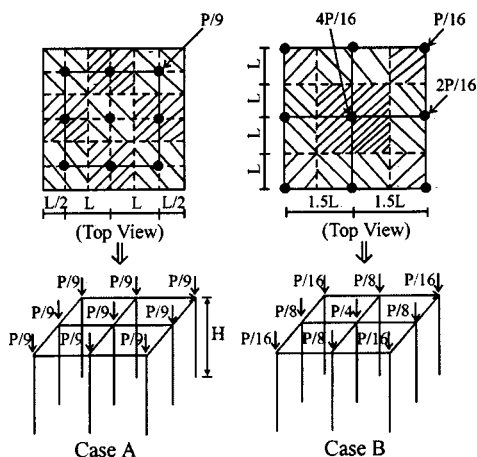


Fig. 4. Arrangement of load case A (average) and load case B (uniform)

Model of Structural Analysis

Shore Arrangement and Boundary Conditions

The load-carrying capacity of a shoring system is varied with the setup of the shores. On construction sites, the distance between the outermost shore of the system and the edge of the formwork placed with fresh concrete induces different reactions on shores. This paper defines load case A as “average load” if the distance between the outermost shore and the slab edge is equal to half of the width between shores. Load case B is defined as “uniform load” if the outermost shore is located at the edge of the slab. Fig. 4 illustrates these two loading conditions for a nine ($=3 \times 3$) shore system.

In load case A, each shore takes a load of $P/9$, and this load condition is termed the average load in this paper. This implies that the total load is evenly distributed to each shore. For load case B, the center shore takes the maximum load, since this shore is assumed to take four portions of load out of the 16 portions of total load. Shores at the corner only share one load portion. The shadowed area in Fig. 4 shows these load distributions.

In this research, all boundary conditions in the analyses are based on the site setup surveyed from actual construction sites in Taiwan. For wood post shores, both the top and the bottom of the shores are linked respectively to the stringers and the ground with even surfaced contacts. A hinge with a spiral spring is assumed at these two boundaries. For metal post shores (i.e., telescopic props), the top and the bottom boundaries are the same as those used in the wood post shores. In addition, the joint between the base and staff tubes is assumed as a hinge with a spiral spring, since this joint is the weakest part of the entire shore. A rigid joint is not appropriate for modeling the structural behavior.

Analysis Modeling

Model of Nonsway Case

This analysis model is used to predict (1) the “modification factor” for the load-carrying capacity of the shoring system; and (2) the “end stiffness” of individual shores. For the modification factor, the load-carrying capacity of a shoring system is different from that calculated from an individual shore based on experimental tests (Peng et al. 1998). In this research, a 3D model is used to predict the modification factor of a shoring system.

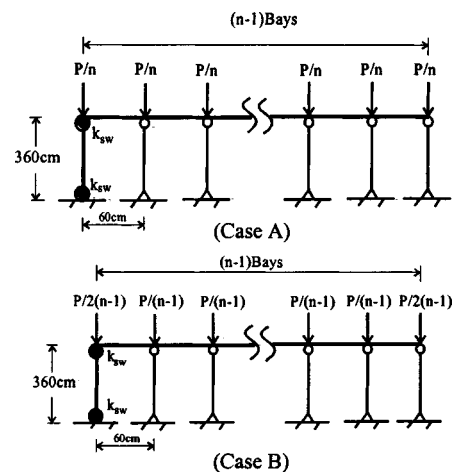


Fig. 5. Analysis models of shoring systems with leaning column effect

In the analysis of the end stiffness of wood and metal post shores, the shore length H is assumed to be 3.6 m, as shown in Fig. 1. The definitions of the end stiffness of the wood and metal post shore are k_{sw} and k_{sb} in Fig. 1. Based on experimental test results, the average stiffness of the joint k_{sm} in the metal post shores is 750 t-cm/rad (7,355 kN-cm/rad) in Fig. 1 (Peng et al. 1998). The end stiffness of the metal post shore can further be predicted when the joint stiffness is defined in the analyses. As shown in Fig. 4, there are two load cases used in the analyses in order to define the end stiffness of wooden and metal post shores. In addition, a simplified 2D model is used to replace a 3D model in order to reduce the computational time.

Model of Sway Case

This analysis model is used to predict (1) the effect of the “leaning column” on the shoring system; and (2) the effect of different positions and numbers of “strong shores” in the shoring system. Owing to the leaning column characteristic in systems, the boundary sway needs to be considered in the analysis model (Aristizabal-Ochoa 1994). To simplify the analyses, a 2D model is used in place of a complicated 3D model. Fig. 5 shows the dimensions of a shoring system with load cases A and B in the analyses, respectively. As shown in Fig. 5, the shores with a pinned-pinned end (i.e., $k_{sw} = 0$) are regarded as leaning columns. The shore with a finite end stiffness (i.e., $k_{sw} \neq 0$) is defined as the strong shore.

Some shores observed on construction sites are combined as a closed-formed system, and other shores are isolated or not sufficiently stiff as a close system. The shores combined as a close-formed system can be considered as an equivalent strong shore, and others are considered as a leaning column. The relationship between the real and equivalent strong shores can be found from experimental tests. For convenience, these equivalent strong shores are termed as strong shores in this paper. The research focuses not only on the effect of leaning columns in the system, but also on the effect of various positions and numbers of equivalent strong shores in the system.

Analysis Results and Discussion

End Stiffness of Shores

Wood Post Shores

Fig. 6 shows the end stiffness of wood post shores, of which the installation is based on the actual setup of construction sites de-

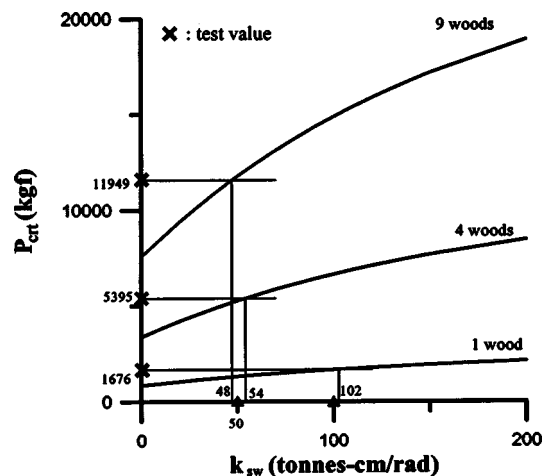


Fig. 6. End stiffness of wood post shores (3.6 m)

scribed above. The length of the shores H is 3.6 m using load case A (Fig. 4). In Fig. 6, the values on the y-axis are the critical loads of the entire shoring systems P_{cr} , and those on the x-axis are the end stiffnesses of wood post shores k_{sw} . The three curves in Fig. 6 express the system critical loads for one-shore, four-shore, and nine-shore shoring systems. The symbol "X" shows the experimental results for the same configurations. The intersections of the horizontal lines passing through X and the theoretical curves represent the corresponding values of the connection stiffness.

As seen in Fig. 6, the end stiffness of the wood post shore is about 100 t-cm/rad (981 kN-cm/rad) for the one-shore case. The end stiffness is about 50 t-cm/rad (490 kN-cm/rad) for both the four-shore case and the nine-shore case. Since the conditions of the four-shore and nine-shore cases are closer to the actual construction site than the one-shore case, the end stiffness of 50 t-cm/rad (490 kN-cm/rad) is more appropriate and is used in the following sections.

In addition, the test result shows that the tested critical loads of shoring systems are lower than those calculated from an individual shore multiplied by the total number of shores in the shoring system (Peng et al. 1998). For example, the average tested critical load of the nine-shore case is 11,949 kgf (117,184 N), which is smaller than 15,048 kgf ($= 9 \times 1,676$) (147,576 N) (Fig. 6). The reduction between the two cases is about 20% [$0.21 = 1 - 11,949 / (9 \times 1,676)$] for the nine-shore case, and $0.20 = 1 - 5,395 / (4 \times 1,676)$ for the four-shore case]. Because the lengths of each shore in the system are not equal, the longer shores will carry a higher load than the other shores when the vertical load is applied to the top of the shoring system. The unequal loading condition fails the portion of shores with higher reaction forces, which subsequently leads to the collapse of the complete system.

In design, each shore in the system is assumed to have the same load-carrying capacity. If the load-carrying capacity of the shoring system is calculated from these individual shores, it will be in the upper bound zone for the strength of the system. Thus, a modification factor is proposed to calibrate the system strength induced from the individual shores. If the modification factor is ignored, an inadequate factor of safety will be designed, and this phenomenon must be prevented. The details of the modification factor are discussed in the next section.

Metal Post Shores

Fig. 7 shows the end stiffness analysis results of metal post shores

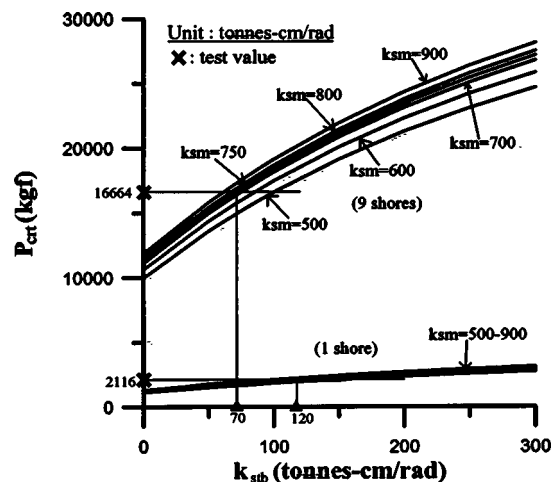


Fig. 7. End stiffness of metal post shores (3.6 m)

with a length of 3.6 m. In the figure, the y-axis shows the critical load of the shoring systems P_{cr} , and the x-axis shows the end stiffness of the metal post shores, k_{sb} . There are two sets of lines in Fig. 7. One is based on analysis of the one-shore case, and the other is from results of the nine-shore case. The stiffness, k_{sm} , is the joint stiffness of the metal post shores. As shown in Fig. 7, the values k_{sb} and k_{sm} change from 0 to 300 t-cm/rad (2,942 kN-cm/rad) and from 500 to 900 t-cm/rad (4,904 to 8,826 kN-cm/rad), respectively. The lines based on the nine-shore case are higher than those of the one-shore case. Since the lines for the one-shore case are very close, the joint stiffness k_{sm} is not listed as in the nine-shore case for clarity.

In the figure, the symbol X on the y-axis shows the experimental test results for the same number of shores. The averaged values are 2,116 kgf (20,752 N) for the one-shore case (Fig. 8) and 16,664 kgf (163,424 N) for the nine-shore case. The end stiffness of the metal post shore is about 120 t-cm/rad (1,177 kN-cm/rad) for the one-shore case and about 70 t-cm/rad (686 kN-cm/rad) for the nine-shore case. Based on the same argument for wood post shores, the end stiffness of 70 t-cm/rad (686 kN-cm/rad) is used for the metal post shores in this paper.

Fig. 9(a) shows the deformed shape of a system of nine metal post shores before and after loading by the numerical analysis. The middle of each shore has the maximum lateral deformation. Fig. 9(b) expresses the load-deflection curves of the shoring system. The y-axis is the vertical load on the shoring system, and the x-axis is the lateral deflection of the central shore. The asymptote to the curve is taken as the critical load of the shoring system.

Modification Factor and Simplified Design Process of Shoring Systems

Modification Factor of Shoring Systems

In the strength design of shoring systems, the load-carrying capacity of an individual shore is first considered. The strength of the individual shores directly chosen from construction sites is commonly measured from tests. The design strength of the entire shoring system is equal to the strength of the individual shore multiplied by the total number of shores. However, based on test results (Peng et al. 1998), the tested load-carrying capacity of the shoring system is always lower than the product of the tested strength of the individual shore and the total number of shores.

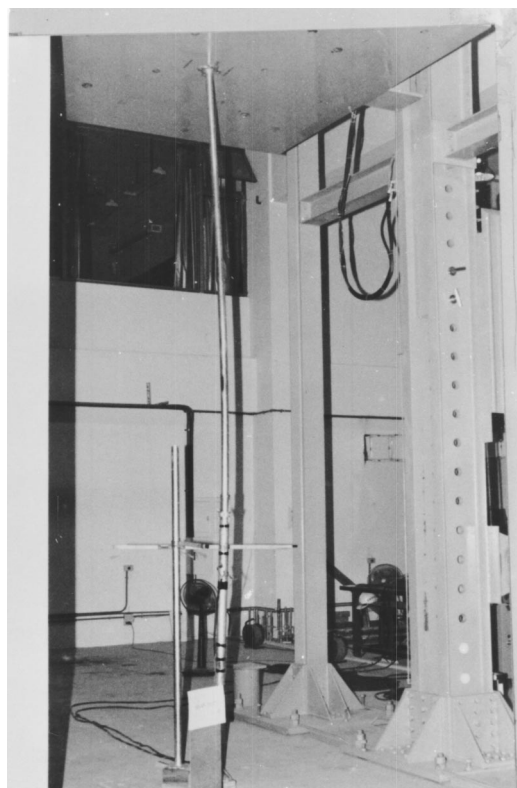


Fig. 8. Experimental test of individual shoring

Thus, a modification factor less than unity should be considered when the strength of a shoring system is computed from individual shores.

Based on test results (Peng et al. 1998), the critical load of the shoring system directly measured from the tests varies from 76 to 80% of the tested critical load of an individual shore multiplied by the total number of shores. As described in the above section, the average value is about 80%. This reduced ratio is defined as the modification factor, ξ_w . For conservatism in design, the factor of $\xi_w = 0.75$ is used for wood post shores in construction in Taiwan. For tested results of metal post shores, the critical load of the shoring system is around 85–88% of the tested strength of an individual shore multiplied by the total number of shores. For conservative design, this paper suggests a factor of $\xi_s = 0.80$ for metal post shores used in construction.

Suggested Design Process of Shoring Systems

Fig. 10 shows numerical, design, and modified design values of wood post shores based on load cases A and B (Fig. 4). The “numerical values” are based on computer calculation, the “design values” are calculated by a simplified design formula, and the “modified design values” are equal to the design values times the above modification factor.

There are four curves in Fig. 10. Curves A and B are the design values based on the two load cases, A and B. They are calculated by the average tested strength of an individual shore multiplied by the shore number of their systems. These two curves can be considered as upper and lower bounds of the strength of shoring systems, respectively. For comparison, a solid curve with symbol (●) is obtained by computer calculation. A dashed curve with symbol (Δ) shows modified design values. The dashed curve is calculated from curve A by multiplying a modification factor $\xi_w = 0.75$. As shown in Fig. 10, the curve of the

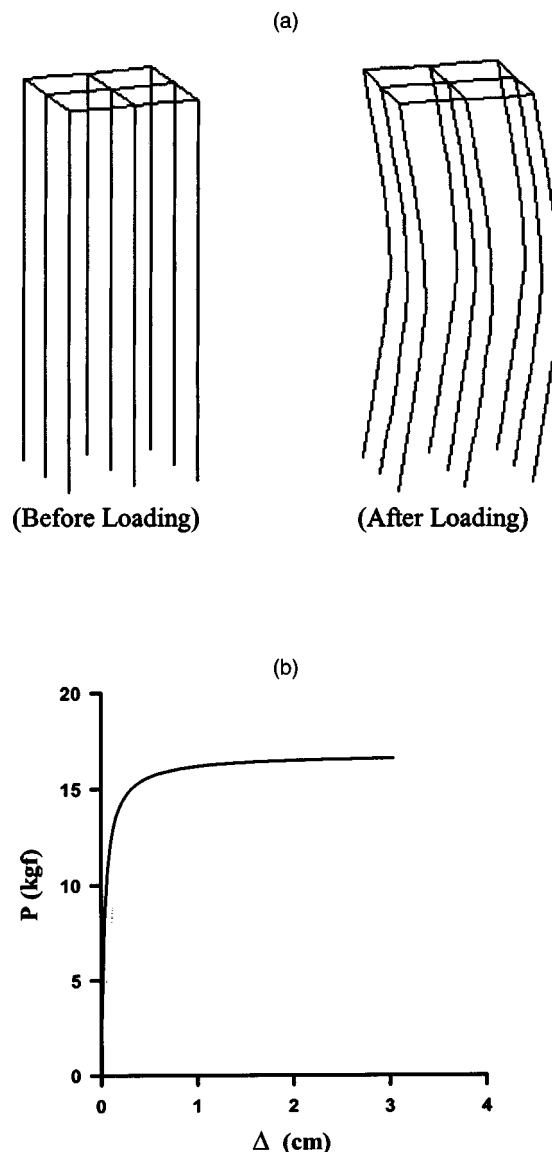


Fig. 9. (a) Deformed shape of nine metal shore system before and after loading; (b) P - Δ curve of nine metal shore system with vertical load

numerical values (●) is close to the curve of the modified design values (Δ). Thus, this modified curve can be considered to replace a time-consuming computer analysis in design. The proposed design formula of the critical loads of shoring systems is summarized as follows:

$$\text{Case A: } P_{crt} = P_{cr} \times m \times n \times \xi \quad (\xi_w \text{ for wood or } \xi_s \text{ for metal}) \quad (8)$$

$$\text{Case B: } P_{crt} = P_{cr} \times (m-1) \times (n-1) \times \xi \quad (9)$$

where m and n = shore number of both sides in the square region of a shoring system; ξ = modification factor of wood or metal post shores; P_{cr} = tested critical load of an individual shore; and P_{crt} = critical load of the entire shoring system.

Design Example

Based on the simplified models as presented above, some design steps are suggested for checking the critical load of a shoring system. It is assumed here that the number of wood post shores is

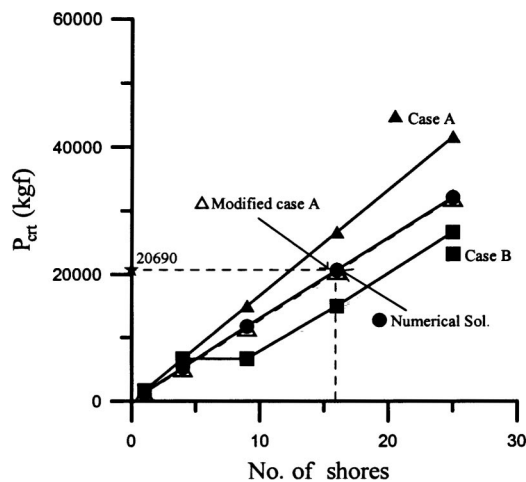


Fig. 10. Critical loads of wood shoring systems

16, and the configuration and layout of the shoring system is square. The design procedure is summarized as follows:

1. Find the tested strength of an individual wood post shore from Fig. 6; 1,676 kgf (16,437 N).
2. Calculate two load cases, A and B, respectively.
 - Case A = $1,676 \times 4 \times 4 = 26,816$ kgf. (262,985 N)
 - Case B = $1,676 \times (4 - 1) \times (4 - 1) = 15,084$ kgf (147,929 N).
3. Multiply using the modification factor $\xi_w = 0.75$.
 - Modified case A = $26,816 \times 0.75 = 20,113$ kgf
 - A = $26,816 \times 0.75 = 20,113$ kgf (197,248 N).
 - Modified case B = $15,084 \times 0.75 = 11,313$ kgf (110,947 N).
4. Check the strength of the 16 shoring systems from Fig. 10; 20,690 kgf (202,907 N) ← (OK).
 - Modified case A = 20,113 kgf ($\approx 20,690$ kgf)
 - ($\approx 20,690$ kgf) ← (suggested).
 - Modified case B = 11,313 kgf ($< 20,690$ kgf).

The modified design value is close to the numerical result, and is more conservative than the design values from the simplified formula. For simplicity, the strength of shoring systems can be determined by this process. Moreover, the load case B can be considered as the lower bound of the shoring system. For structures with higher headroom or thicker slabs, load case B can be

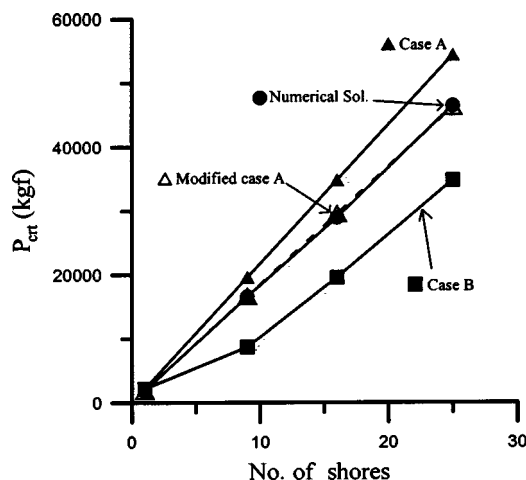


Fig. 11. Critical loads of metal shoring systems

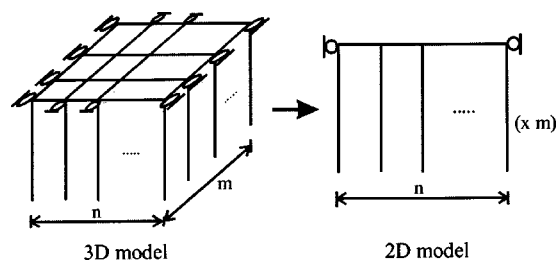


Fig. 12. 3D and simplified 2D models in analyses

used. In addition, the above procedure provides a quick and simple means to find the system strength of wood post shores. Design of various numbers of shores can also adopt the procedure.

Fig. 11 shows numerical, design, and modified design values of metal post shores by two load cases, A and B, in a procedure similar to that for wood post shores. The trends of these four curves are very similar to those in Fig. 10. The design system strength of metal post shores can be calculated by considering Figs. 7 and 11, based on the above design process.

Simplified 2D Model

A simplified 2D model is proposed to replace a complex 3D model. Fig. 12 shows this 2D shoring system simplified from a 3D system, based on the model of the nonsway case mentioned above. Fig. 13 expresses the analysis results of these two models by load case A. As shown in Fig. 13, the analysis of the simplified 2D model is very close to that of the 3D model. Thus, the following analyses are based on this kind of 2D model.

Leaning Column Effect and Suggestions of Shore Design

Wood Post Shores

This paper proposes the consideration of the leaning column effect on wood shoring systems in this section. For simplicity, a strong shore with an end stiffness of $k_{sw} = 50$ t-cm/rad (490 kN-cm/rad) and leaning columns is considered in this parametric

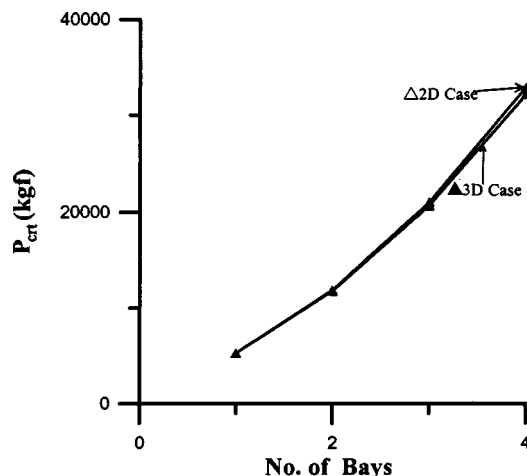


Fig. 13. Comparison of analysis results of 2D and 3D models

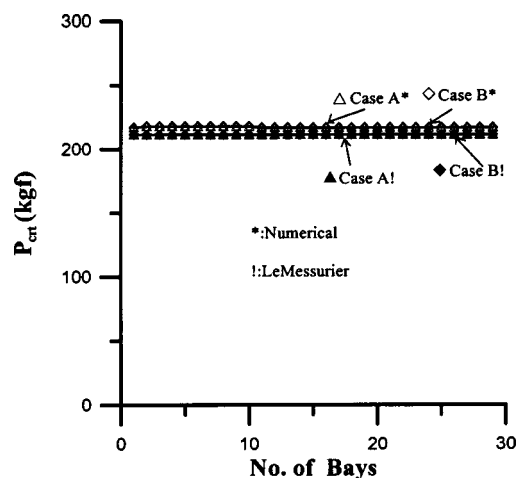


Fig. 14. Critical loads of wood shoring systems versus number of bays of leaning columns (one strong shore)

analysis. The LeMessurier formula (LeMessurier 1977) can be written for the effective length factor, K , as

$$K = \sqrt{\frac{P_e}{P_i} \times \frac{\Sigma P}{\Sigma P_{ek}}} \quad (10)$$

where P_e =Euler load; P_i =axial force in the column providing sidesway resistance; ΣP =total axial load on all columns in a story; and ΣP_{ek} =summation of the Euler buckling load of all columns in a story providing sidesway resistance, which can be evaluated using the effective length obtained from nomographs by Chen and Lui (1988).

Fig. 14 shows results for different numbers of bays by using the computer and by the LeMessurier formula. The stiffness of a horizontal beam is considered as rigid when compared to that of vertical shores, based on actual construction conditions. This is due to the stiffness of the whole formwork being very strong when compared to each individual shore surveyed from actual construction sites. In computer analyses, the beam stiffness assumes 1,000 times that of shores to simulate the rigidity. The end stiffness of wood post shores is 50 t-cm/rad (490 kN-cm/rad), as mentioned above. The height of the shores is 360 cm and the distance between the shores is 60 cm for load cases A and B, based on the actual setup on construction sites.

Fig. 14 expresses the relationship between critical loads and the bay numbers of leaning columns in shoring systems. In the figure, the y-axis shows the system critical loads of the shoring systems P_{cr} , and the x-axis shows the bay numbers of leaning columns in shoring systems. There are four curves in Fig. 14. Two curves are plotted from the computer results by load cases A and B. The other two curves are based on the LeMessurier formula, also by load cases A and B. As shown in Fig. 14, the solutions of the LeMessurier formula are slightly lower than the computer solutions. This indicates that the LeMessurier design formula can substitute for cumbersome numerical analyses by computers.

In the above setup, when the number of strong shores is fixed, the critical load of shoring systems approaches a constant, irrespective of the increase in the number of leaning columns. This result is valuable in verifying the safety of shoring systems on actual construction sites. During construction, workers need to realize whether the added shores are of contribution to the system stability or not. If only the leaning columns are added in the

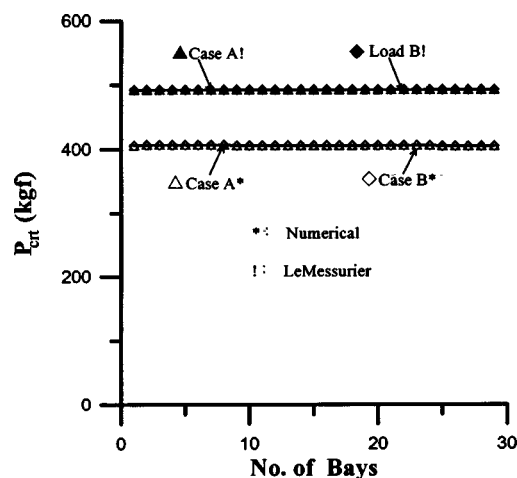


Fig. 15. Critical loads of metal shoring systems versus number of bays of leaning columns (one strong shore)

systems, the system critical loads will not increase. The shoring systems still have a potential danger. If the workers do not realize this behavior, it may lead to the collapse of shoring systems on construction sites.

Metal Post Shores

To study the leaning column effect on a metal shoring system, the analysis process is similar to that for wood post shores. In the analysis, the end stiffness of metal post shores is taken as 70 t-cm/rad (686 kN-cm/rad), based on the above derivation, and the stiffness of joints in metal post shores is 750 t-cm/rad (7,355 kN-cm/rad), based on experimental tests (Peng et al. 1998).

Fig. 15 shows the relationship between critical loads of shoring systems and the bay numbers of leaning columns for a metal shoring system. The definitions of the y-axis and x-axis are the same as those for the wood post shores. In Fig. 15, when the number of strong shores is fixed and the number of leaning columns increases, the critical load of shoring systems remains constant. This result resembles that for wood post shores (Fig. 14). In addition, the solutions derived from the LeMessurier formula are larger than those from numerical analyses. Due to the ignorance of the joint stiffness of metal shores, the LeMessurier formula predicts a much higher critical load. Designers should, therefore, be careful when using the LeMessurier formula for metal post shores in design.

Quantities and Positions of Strong Shores—Suggestion for Shore Design

Wood Post Shores

Number of Strong Shores

The effect of leaning columns is required to be considered when the bound of the system has sidesway. This paper investigates the leaning column effect on shoring systems with various numbers of strong shores. In the analysis, the total number of wood post shores is fixed at 30. Fig. 16 shows the relationship between critical loads of wood shoring systems and the number of strong shores. There are two curves based on the LeMessurier formula and numerical analyses with load case A in the figure. Fig. 16 shows that these two curves are very close. This implies that the

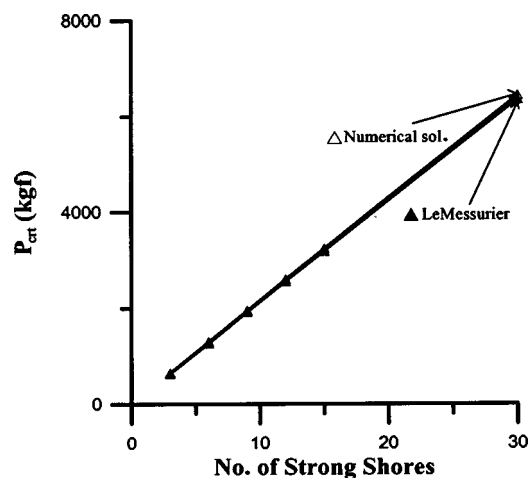


Fig. 16. Critical loads of wood shoring systems versus number of strong shores with leaned column effect (30 shores)

LeMessurier formula can be used to replace the complex numerical computing work in this condition for the shore design.

As shown in Fig. 16, the critical loads of shoring systems P_{cr} increase linearly with the number of strong shores. This result is useful in the strength design of shoring systems in construction. Based on this result, critical loads of other systems with various numbers of strong shores can be interpolated from the curves.

Ratios of Strong Shores

Fig. 17 demonstrates the relationship between critical loads of shoring systems and the ratios of strong shores in various shoring systems. Three curves are based on various numbers of shores—10, 20, and 30. As shown in Fig. 17, these three curves increase linearly with the increase of the ratios of strong shores. In addition, the strength of shoring systems increases with the increase of the total number of shores when the ratios of strong shores are equal.

By interpolation, Fig. 17 is applicable to different shore numbers. For example, if the total number of shores is 25 and the ratio of strong shores is 0.4, the following procedure can be used to determine the strength of the shoring system. From Fig. 17, the linear curve for 25 shores can be found by interpolating between

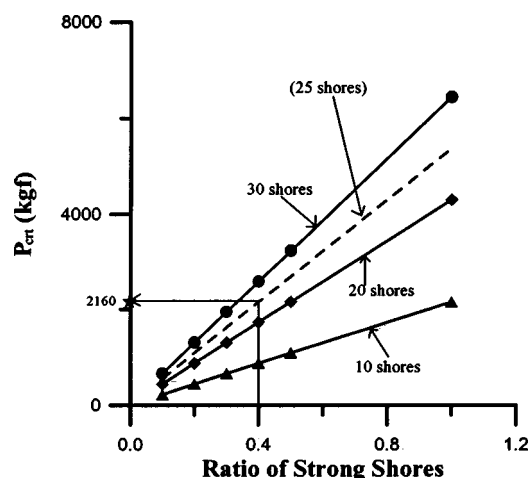


Fig. 17. Critical loads of various wood shoring systems versus ratios of strong shores with leaned column effect

Positions of Strong Shores	P_{cr} (kgf)
	651.4
	651.4
	651.5
	651.5

Fig. 18. Relations between critical loads of wood shoring systems and various positions of strong shores with leaning columns

20 shores and 30 shores by a dashed line. With the ratio of strong shores equal to 0.4, the strength of the 25-shore system equal to 2,160 kgf (21,183 N) can be found on the y-axis.

From the above, Fig. 17 can provide a quick prediction for the system strength of wood post shores. Furthermore, based on assumptions in this paper, the system critical load of wood post shores increases linearly with the increase of the number of strong shores. For the analysis and design of the shoring system, the critical loads of the entire shoring system can be found by multiplying the strength of an individual strong shore by the total number of strong shores. Fig. 17 is very helpful in shore design.

Positions of Strong Shores

Based on the leaning column effect in shoring systems from actual construction sites, the change of positions of strong shores does not have an apparent influence on the critical load of the shoring system. In Fig. 18, a system of 10 shores with three strong shores is considered. Based on actual setups on construction sites, the length of the shores is 3.6 m and the distance between the shores is 60 cm. The end stiffness of strong shores k_{sw} is 50 t-cm/rad (490 kN-cm/rad). Fig. 18 shows that critical loads of the shoring systems almost do not change with the different positions of strong shores. This implies that the positions of strong shores are unimportant to the strength of a shoring system. For a one-layer shoring system on construction sites, workers should therefore be reminded of the importance of the number of strong shores, but not their locations.

Metal Post Shores

Fig. 19 shows the relationship between critical loads of a metal shoring system and the number of strong shores. In the figure, the total number of shores is also equal to 30. As shown in the figure, except for the larger discrepancy between the two curves, the trend of the curves increases linearly with the increase of the

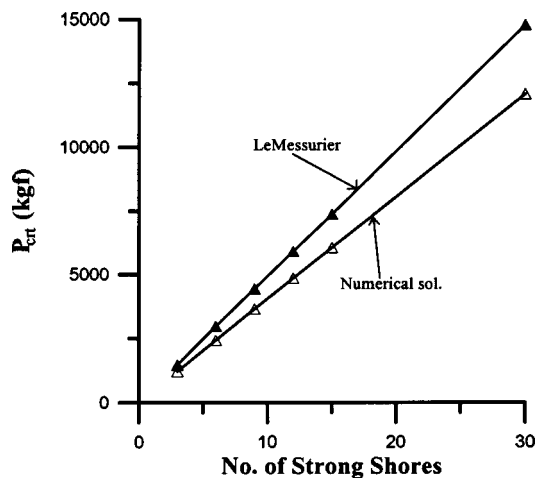


Fig. 19. Critical loads of metal shoring systems versus number of strong shores with leaned column effect (30 shores)

number of strong shores. The numerical analyses have taken into account a joint stiffness of metal post shores of 750 t-cm/rad (7,355 kN-cm/rad), obtained from experimental tests (Peng et al. 1998). However, the rigid joint ($k_{sm} = \infty$) assumption is used in the calculation with the LeMessurier formula. This is the reason for a higher value computed by the LeMessurier formula when compared to the numerical analysis results in Fig. 19.

Conclusions

The following conclusions can be drawn from the studies:

1. From observations of actual construction sites, the length of the shores is assumed to be 3.6 m, the tops of the shores are linked to the stringers, and the bottoms of the shores rest on existing concrete slabs on grade. The end stiffness of shores should be taken as 50 t-cm/rad (490 kN-cm/rad) for wood post shores and 70 t-cm/rad (686 kN-cm/rad) for metal post shores for stability analyses.
2. If the shore design is based on an individual shore and the factor of safety is ignored, the modification factors of $\xi_w = 0.75$ for wood post shores and $\xi_s = 0.85$ for metal post shores are recommended in the system without the leaning column effect. For simplicity, the critical loads of shoring systems are equal to the tested critical load of the individual shore multiplied by the total number of shores and the modification factor.
3. The strengths of shoring systems are based on the number of strong shores in the system. The system strength will not increase by an increase in the number of leaning columns. In construction, the shores need to be distinguished between strong shores and leaning columns, since leaning columns are useless for the strength of the shoring system. This is the main reason for collapse of falsework, since workers do not normally realize this characteristic during construction.
4. For simplicity, the LeMessurier formula for wood post shores can be used to replace the complex numerical analysis. However, this approach is unconservative for metal post shores, since the joint stiffness is assumed rigid.

5. The critical loads of shoring systems increase linearly with the increase in the number of strong shores. On construction sites, appropriately fastening individual shores as strong shores is a crucial point for improving the strength of the complete shoring system.
6. In the simplified shore design, if the total number of shores and the ratio of strong shores are known, the critical load of the shoring system can be approximated by interpolation.
7. If the total number of shores is fixed, the critical loads of shoring systems are almost independent of the positions of strong shores.

Acknowledgments

The writer acknowledges Professors S. L. Chan of the Hong Kong Polytechnic University and W. F. Chen of the University of Hawaii for their invaluable comments. The writer also thanks graduate students W. C. Huang and C. H. Kung for their help in the tests. The financial support provided by the National Science Council (NSC 89-2211-E-224-037) in Taipei, Taiwan is greatly appreciated.

Appendix. Conversion Factors

To convert from inches to centimeters, multiply by 2.54. To convert from kilogram-force (kgf) to newtons, multiply by 9.807. To convert from tons to kilonewtons, multiply by 9.807. To convert from kip to kilonewtons, multiply by 4.448.

References

- Aristizabal-Ochoa, J. D. (1994). "Slenderness K factor for leaning columns." *J. Struct. Eng.*, 120(10), 2977–2991.
- Chan, S. L., and Zhou, Z. H. (1994). "A pointwise equilibrium polynomial (PEP) element for nonlinear analysis of frame." *J. Struct. Eng.*, 120(6), 1703–1717.
- Chen, W. F., and Lui, E. M. (1988). *Structural stability: Theory and implementation*, Elsevier Science, New York.
- Chen, W. F., and Mosallam, K. H. (1991). *Concrete buildings: Analysis for safe construction*, CRC, Boca Raton, Fla.
- Council of Labor Affairs. 1997. "Investigations of construction accidents: 1993–1995." IOSH86-03. *Research Rep.*, Taipei, Taiwan (in Chinese).
- El-Shahhat, A. M., Rosowsky, D. V., and Chen, W. F. (1994). "Construction safety of multistory concrete buildings." *ACI Struct. J.*, 91(4), 475–485.
- LeMessurier, W. J. (1977). "A practical method of second order analysis. Part 2—Rigid frames." *AISC Eng. J.*, 14(2), 49–67.
- Peng, J. L., Huang, W. C., and Kung, C. H. (1998). "Load-carrying capacity of one-layer falsework systems." *Structural Engineering Rep. CE-98-05*, Chaoyang Univ. of Technology, Taichung, Taiwan (in Chinese).
- Peng, J. L., Rosowsky, D. V., Pan, A. D., Chen, W. F., Chan, S. L., and Yen, T. (1996). "High clearance scaffold systems during construction. Part II: Structural analysis and development of design guidelines." *Eng. Struct.*, 18(3), 258–267.
- Peng, J. L., Yen, T., Lin, I., Wu, K. L., and Chen, W. F. (1997). "Performance of scaffold frame shoring under pattern loads and load paths." *J. Constr. Eng. Manage.*, 123(2), 138–145.